Atmos. Chem. Phys. Discuss., 11, 18487–18525, 2011
www.atmos-chem-phys-discuss.net/11/18487/2011/
doi:10.5194/acpd-11-18487-2011

Atmospheric Chemistry and Physics Discussions

Scattering and absorption by aerosols during EUCAARI-LONGREX: can airborne measurements and models agree?

E. J. Highwood[1], M. J. Northway[1], G. R. McMeeking[2,*], W. T. Morgan[2], D. Liu[2], S. Osborne[3], K. Bower[2], H. Coe[2], C. Ryder[1], and P. Williams[2]

[1]Department of Meteorology, University of Reading, Reading, UK
[2]SEAS, University of Manchester, Manchester, UK
[3]Met Office, Cardington, UK
[*]now at: Department of Atmospheric Science, Colorado State University, USA

Received: 27 April 2011 – Accepted: 13 June 2011 – Published: 29 June 2011

Correspondence to: E. J. Highwood (e.j.highwood@reading.ac.uk)

Published by Copernicus Publications on behalf of the European Geosciences Union.

Abstract

Scattering and absorption by aerosol in anthropogenically perturbed air masses over Europe has been measured using instrumentation flown on the UK's BAe-146-301 large Atmospheric Research Aircraft (ARA) operated by the Facility for Airborne Atmospheric Measurements (FAAM) on 14 flights during the EUCAARI-LONGREX campaign in May 2008. The geographical and temporal variations of the derived shortwave optical properties of aerosol are presented. Values of single scattering albedo of dry aerosol at 550 nm varied considerably over the data set from 0.86 to near unity. Dry aerosol optical depths ranged from 0.03 to 0.24. An optical properties closure study comparing calculations from composition data and Mie scattering code with the measured properties is presented. Very good agreement (to within 30 %) can be achieved for scattering, but the modelling of absorption is shown to be sensitive to the refractive indices chosen for organic aerosols, and to a lesser extent black carbon. Agreement with the measured absorption can only be achieved if organic carbon is assumed to be only weakly absorbing. Hygroscopic growth curves derived from the wet nephelometer indicate moderate water uptake by the aerosol with a campaign mean f(RH) value (change in scattering) of 1.3 at 80 % relative humidity. This value is consistent with the major chemical components of the aerosol measured by the aerosol mass spectrometer (AMS), which are primarily mixed organics and nitrate and some sulphate. As expected the effect of humidity is to raise the single scattering albedo, and to increase the aerosol optical depth. This study represents an important new body of data regarding European aerosol amounts, composition and optical properties and additionally demonstrates the importance of airborne measurements of black carbon mass and aerosol hygroscopicity.

ACPD

11, 18487–18525, 2011

1 Introduction

Atmospheric aerosol has a "direct effect" on climate through the scattering and absorption of radiation and "indirect effects" via changes to cloud microphysics and properties. These effects are potentially considerable but uncertain. The global mean direct radiative forcing from 1750 to 2005 due to all aerosol was estimated as $-0.5+/-0.4\,\mathrm{Wm}^{-2}$and the indirect effect as -0.7 (with a range from -1.1 to $0.4)\,\mathrm{Wm}^{-2}$ (IPCC, 2007) Aerosol plays a particularly important role in producing regional radiative forcing (although this can have non-local climate impacts). In order to estimate the direct effect of any aerosol we must know their optical properties. At the most basic level this means being able to quantify the refractive index (itself a function of composition) as a function of wavelength, the size distribution, the influence of relative humidity and the mixing state (internal or external). These properties are also included in or predicted by aerosol transport models and regional and global climate models and used in satellite retrieval algorithms for aerosol optical depth or other quantities. Climate models generally require the mass extinction co-efficient, single scattering albedo, phase function (or its simplified form the asymmetry parameter) as well as the hygroscopicity. In order to include the indirect effects, size distribution and activation information are also required. All of these properties are a complex function of aerosol size, composition, and chemical and physical processing (including relative humidity and clouds where these occur).

Some models that include aerosol interactively compute internally the size distribution or loading of aerosol types and determine the radiative effect using Mie scattering code or similar approaches. Others will prescribe bulk aerosol optical properties based on measurements from field campaigns or derived measurements such as those from the AErosol RObotic NETwork (AERONET). Volume weighted mixing is often used to combine optical properties (for external mixtures) or refractive indices and density prior to scattering calculations (for internal mixtures) of aerosol components such as sulphates or black carbon (BC) (e.g. Chylek et al., 1988; Osborne et al., 2007; Cook et

ACPD
11, 18487–18525, 2011

al., 2007). It is important to quantify the uncertainty with which we know firstly the refractive indices of individual aerosols as measured in the laboratory, and secondly how mixing the components affects scattering and absorption. Several studies have examined closure of these properties, where measured values of scattering and absorption were compared with calculations of the same using chemical composition information, measured particle size and a scattering code (e.g. Cai et al., 2011; Scaiare et al., 2005; Wex et al., 2002; Quinn and Coffman, 1998). However, for aerosol including absorbing black carbon, this has not previously been possible from the UK's BAe-146-301 large Atmospheric Research Aircraft (and rare on other airborne platforms) since measurement of BC mass has only been possible by analysing filter samples post-flight. Particularly in situations with low BC amount, the resulting BC mass has a large uncertainty associated with it. As a result, the amount of BC used in the "model" aerosol has often been tuned to give closure on single scattering albedo as measured directly using aethelometer-type instruments (e.g. Cook et al., 2007; Osborne et al., 2007) – using filter measurements only to check the consistency of the mass of BC required. This procedure is particularly prone to uncertainty as the refractive index of black carbon is difficult to define and depends on source, processing and age of the aerosol.

The advent of the SP2 instrument (Stephens et al., 2003; Schwarz et al., 2006) on board the FAAM BAe-146 (McMeeking et al., 2010) has allowed consistent measurements of the mass of BC to be used alongside those of sulphates, organics and nitrates taken from the Aerosol Mass Spectrometer (AMS). For the first time from this platform we are then able to perform optical property closure studies without tuning the black carbon amount, and to quantify the degree to which we can bring models and measurements of aerosol scattering and absorption into agreement. Another recent addition to the FAAM BAe-146 platform, the wet nephelometer, allows further new possibilities for closure studies for aerosol optical properties in the ambient/wet environment. This study therefore presents a significant new body of data concerning hygroscopic and optical properties of aerosol in anthropogenically perturbed airmasses. It should be noted that this combination of measurements is particularly appropriate

ACPD
11, 18487–18525, 2011

for anthropogenic aerosol where the majority of aerosol mass can now be measured. Since the AMS only measures the non-refractory component and the SP″ only measures material that is sufficiently light absorbing at 1064 nm, in regions where sea salt or mineral dust are a large contributor to the aerosol, closure studies would still require further instrumentation for full chemical resolution.

The FAAM BAe-146 data from the EUCAARI-LONGREX campaign presents a novel opportunity to explore the agreement between models and airborne measurements of optical properties for an anthropogenic aerosol of a variety of ages across north-west Europe. Section 2 of this paper describes briefly the campaign meteorology, flights undertaken and instrumentation used. Section 3 presents the optical properties derived from the airborne measurements. Section 4 discusses measurement of the increased scattering by aerosol due to relative humidity and its effect on measured aerosol properties. Section 5 discusses Mie scattering calculations using chemical composition and size distribution and the success of optical closure experiments. The work is summarized and conclusions are drawn in Sect. 6.

2 Flights and instrumentation

2.1 EUCAARI meteorology and flights

During the EUCAARI-LONGREX campaign of May 2008, the FAAM Bae-146 made around 14 flights generally consisting of 5 h sorties over central Europe or off the coast of the UK. The flights used in this paper (defined in Table 1) span the region 47–57° N and 12° W to 22° E and aimed to probe both the boundary layer and free troposphere in clean and polluted conditions. Flight patterns generally consisted of either north-south transects to cut across air mass gradients or east-west transects to follow the air mass trajectories. Aircraft manoeuvres included straight and level runs (SLRs) at a variety of altitudes within and above the boundary layer and deep profiles through the boundary layer at rates of 5 ms^{-1} above the boundary layer and 2.5 ms^{-1} within the boundary

ACPD
11, 18487–18525, 2011

layer.

The meteorology of the EUCAARI-LONGREX campaign has been discussed extensively in Morgan et al. (2010a,b), McMeeking et al. (2010) and Hamburger et al. (2010) so will not be repeated here in detail. The majority of flights took place during a period dominated by a strong high surface pressure system positioned in the region of Denmark. Following Morgan et al. (2010), the EUCAARI LONGREX period can be divided into 3 parts based on the dominant meteorology: LONGREX-1 (6–8 May 2008, flights B362–366) is defined by approximately zonal flow from east to west; during LONGREX-2 (10–14 May 2008, flights B369–B374) the strong anticyclone was centered over Denmark and northern Germany resulting in more strongly curving anticyclonic flow; whilst finally LONGREX-3 (19–20 May, flights B379–380) was characterized by building high pressure following the passage of a weak frontal system across northern Europe with predominantly easterly flow. As a representative example of the flow during the majority of the flights discussed in this paper, Fig. 1 shows the synoptic situation during the LONGREX-2 period as defined by the mean sea level pressure from ECMWF analyses at 12:00 UTC on 13 May 2008. Flights during LONGREX2 in particular were designed to follow the airmass from east to west across north-western Europe, sampling increasingly aged aerosol as well as that from local sources, such that any influences of aging/transport/emissions on optical properties and chemical composition might be determined.

2.2 Instrumentation

The FAAM BAe-146 carries a considerable range of instrumentation. Only the instrumentation particularly relevant for optical property studies is described here – more comprehensive discussion of the full instrumentation can be found in Johnson et al. (2000) and Osborne et al. (2007). Table 2 summarises the instruments, standard processing, and associated references used in this study. Of particular note are the corrections made to the TSI 3563 nephelometer and PSAP data as discussed by Anderson and Ogren (1998) and Bond et al. (1999) including the clarification by

ACPD
11, 18487–18525, 2011

Ogren (2010). The Compact Time-of-flight Aerosol Mass Spectrometer (cToF-AMS), Aerodyne Research Inc (Drewnick et al., 2007) , Particle Soot Absorption Photometer (PSAP), dry and humidified nephelometers, and Single Particle Soot Photometer (SP2) instruments were sampled using Rosemount inlets. These inlets have not been fully characterized on the FAAM BAe-146, but recent studies have suggested that for general sampling conditions of the aircraft and instrumentation the inlet has an upper size cut-off of approximately 3 µm optical diameter (McConnell et al., 2008; Haywood et al. 2003). From these data, optical properties can be derived as follows.

2.2.1 Specific mass extinction co-efficient at 0.55 µm

The mass-specific extinction co-efficient (k_e, units $m^{-2}\,g^{-1}$) can be determined by considering the relationship between the total mass of aerosol measured by the AMS and SP2 instruments and the measured extinction from the nephelometer and PSAP. The extent to which the AMS mass represented the submicron mass was checked by comparison with the volume convolved number size distribution from the passive cavity aerosol spectrometer probe (PCASP), a wing-mounted optical particle counter, and shown to agree to within 30 % on average across the campaign (Morgan et al., 2010a). Uncertainty in the measured extinction has been calculated from uncertainties in scattering and absorption as measured by the nephelometer and PSAP instruments respectively. Here we have estimated the measurement uncertainty in scattering as 20 % and in the absorption as 30 % based on a wing-tip to wing-tip comparison with a second research aircraft that also participated in the campaign, the DLR-Falcon, as described fully in McMeeking et al. (2010). Uncertainty in run averaged quantities used here also derive from variability experienced during the 15 min SLRs. The average in-run variability of scattering from the nephelometer during the ranged from 12 % for B370 to 34 % for B364. For the PSAP absorption measurements, the in-run variability was generally considerably higher, ranging from 16 % for B368 to 48 % for B365. Combining these sources of uncertainty results in an average error of around 30 % in the measured scattering and 50 % in measured absorption. The uncertainty in extinction

ACPD
11, 18487–18525, 2011

(25 %) is closer to that in scattering since the absorption is only a small component for this aerosol.

2.2.2 Single scattering albedo (SSA) at 0.55 µm

The single scattering albedo (SSA) is defined as the ratio of scattering to the total extinction of radiation by the aerosol defined for a particular wavelength. The wavelength of 0.55 µm is widely used in aerosol studies since it is near the peak of the visible solar radiation spectrum. Additionally the degree of scattering of radiation is strongest at a wavelength comparable to its radius. Most atmospheric aerosols, with the possible exceptions of mineral dust, some volcanic ash and sea salt, have volume distributions peaking below 1 µm, therefore 0.55 µm captures representative optical effects.

As indicated in Table 2, the scattering measured by the nephelometer is for aerosol at low relative humidity since the sample flow is not actively dried but is at lower than ambient relative humidities, due to the heat provided by its electronics, lamp, the dynamic heating through deceleration of the input flow which reaches the instrument and the increased temperature of the sample lines compared to ambient air. The sample flow humidity is actually dependent on the ambient relative humidity and in cases where the ambient relative humidity (RH) is high this may lead to the sample being only drier than the ambient air rather than absolutely dry. To minimize the impact of this uncertainty, only sections where the RH measured in the dry nephelometer is less than 30 % have been used to calculate the growth factors for scattering described in Sect. 4. If the nephelometer RH was larger than this, the growth curve resulting from dry sections of the flight has been used to adjust the scattering co-efficient to that expected at 20 % RH. In most runs considered here, this effect was very small. The nephelometer and PSAP measurements are combined with consideration of RH effects to calculate the "dry" single scattering albedo (ω_{dry}) at 0.55 µm. This is calculated for all straight and level runs (SLR) for each of the flights. Using the estimated uncertainties in measured extinction and scattering results in around a 40 % uncertainty in SSA. In Sect. 4, the "ambient" single-scattering albedo ω_{amb} is calculated using the

ACPD
11, 18487–18525, 2011

non-humidified nephelometer and the growth factor derived from the humidified nephelometer.

2.2.3 Aerosol optical depth

The aerosol optical depths (AODs) are retrieved by integrating the extinction profile, generally taken as the sum of the aerosol scattering and aerosol absorption. Because of problems with the PSAP instrument pressure regulation during the campaign, many segments of the aircraft ascents and descents (particularly) were not usable. Thus, for AOD calculations, only the scattering coefficient profiles were integrated. The error introduced by neglecting absorption is small in this campaign since the PSAP values are often of the order of 1 % of the nephelometer values (see Sect. 3.2). Some profiles cover a restricted altitude range (in particular, aerosol near the ground is not likely to have been measured) and this can lead to the AOD calculated in this study being a lower bound. It is also important to remember that since the profiles are performed in an aircraft having a finite ascent and descent rate, the aircraft may cover a few hundred kilometers in the horizontal during each profile, depending on the flight pattern. If there is substantial horizontal variability in aerosol profile, this can lead to potentially unrealistic averaging of the aerosol. Assuming that the horizontal variability experienced during profiles is similar to that observed during 15 min SLR runs, the uncertainty in scattering is around 30 % and this results in an uncertainty of 30 % in optical depth estimated by this method.

2.3 Scattering code

A Mie scattering code as released alongside the Edwards and Slingo (1996) radiative transfer code (hereafter ES96) is used to calculate absorption and scattering from the SLR mean refractive indices and size distributions for each run and each flight.

ACPD
11, 18487–18525, 2011

3 Results: measured optical properties

In this section, the nephelometer, PSAP, AMS, SP2 and PCASP data are used as described in Sect. 2.2 to describe the radiatively relevant properties of dry aerosols across north-west Europe.

3.1 Mass extinction co-efficient

Figure 2 shows the total extinction (sum of scattering from nephelometer and PSAP) as a function of total mass of submicron aerosol (combined from AMS and SP2). The extinction is dominated by scattering. The campaign mean mass extinction co-efficient for dry aerosol (given by the slope of the best fit line in Fig. 2) is $4.6 \pm 1.9\,m^2\,g^{-1}$ (at 550 nm) – the uncertainty here is derived from the average residual from the best line fit shown in Fig. 2. The estimated errors in extinction as derived from the measurements and described in Sect. 2 are also shown and range between 20 and 30 % for the majority of the flights. Morgan et al. (2010a) report the scattering co-efficient of ambient aerosol derived using a similar analysis for a sub-sample of the flights to be $4.94\,m^2\,g^{-1}$. These values are consistent since the scattering co-efficient would be expected to increase with relative humidity. Bates et al. (2006) give a somewhat lower value for submicron aerosol sulphate/carbonaceous aerosol over the N. Atlantic of $3.66\,m^2\,g^{-1}$. Again this value is consistent with that found here since there is a relatively large proportion of ammonium nitrate in much of the north-west European aerosol (e.g. Morgan et al., 2010), and this is highly scattering. The ADRIEX campaign in Northern Italy using the same measurement platform (but a different methodology and some different instrumentation) found a value of $3.5+/-1.2\,m^2\,g^{-1}$ for ambient industrial aerosol also with a large nitrate component (Osborne et al., 2007), which is consistent with our value within the measurement uncertainties.

Figure 2 also shows a clear increase in extinction during the LONGREX-2 period (flight B368 in "fresh" aerosol to flight B374 in "aged aerosol"). However there is little to distinguish the three different LONGREX periods from each other.

ACPD
11, 18487–18525, 2011

3.2 Single scattering albedo (SSA)

Figure 3 shows the measured single scattering albedo (dry aerosol) across Europe as defined by the mean across each straight and level run. It is clear from Fig. 3a that the SSA for dry aerosol across NW Europe is relatively high, generally exceeding 0.93. Values of 0.9 and lower are generally restricted to regions very close to fresh sources. The highest values are seen in flights over the North Sea and west of Ireland. Flight and campaign average SSA is shown in Table 3 for two regions of vertical profiles, "LOWLEV" – below 250 m and "BL" – boundary layer between 250m and 2000m. Above this altitude, aerosol amounts were generally low and hence large uncertainties are introduced in the nephelometer and PSAP measurements. BL values for dry aerosol range from 0.92 to 0.94 with the exception of one flight (B368) which shows a much smaller SSA of 0.7. This flight was in a very different location to all the others, being in the eastern Baltic Sea. Local pollution sources are likely to be different there, although the mass loading of BC was the smallest observed. These values must therefore be treated with some caution. The "Lowlev" runs for B362, B365, B369 and B74 all show a considerably higher SSA than the BL runs for the same flights. All these low level runs were over water, and the presence of sea salt might explain the higher dry SSA. The AMS measurements also show enhanced ammonium nitrate in moist layers close to the sea surface and this would also contribute to a higher SSA. In contrast, the low level SSA for B380 is lower than the BL value. This run was completed just off the south coast of the UK and the AMS data shows relatively high amounts of sulphates, organics and BC and relatively little highly scattering nitrate, suggesting a local pollution source and consistent with a low SSA.

Using the estimation of 40 % uncertainty in SSA as discussed in section 2, the campaign average SSA (excluding B368) is 0.93 ± 0.37. The relatively high value reflects the large proportion of scattering material (sulphate, nitrate and organics) in EU anthropogenically influenced aerosol. The uncertainty range is larger than quoted in other similar studies, and indeed the narrow range of values seen across the campaign

ACPD
11, 18487–18525, 2011

suggest that this value is an over-estimate. During LONGREX-2 (10–14 May, flights B369–B374, following Morgan et al., 2010a) the flow is essentially from north east to south west following the air mass circulating around the southern side of the anticyclone and therefore sampling progressively aged aerosol from flight B369–B374. However, when SSA is plotted as a function of longitude (not shown), and considering the uncertainty in SSA calculated above, no immediate relationship with longitude is apparent. Increased SSA is found preferentially in regions of increased nitrate, these being generally to the west of the domain and also over Belgium and the Netherlands where there are strong emissions of nitrate pre-cursors. This dependency of SSA on nitrate mass has also been observed within the context of a single flight (Morgan et al., 2010a). These findings have important implications for the calculations of radiative forcing since nitrate has yet to be included in many aerosol transport models and GCM aerosol schemes.

3.3 Vertical profile and optical depth

Figure 4a shows the variation of dry AOD derived as described in Sect. 2.2.3. The values estimated for the most complete profiles used are shown in Table 4. Typical vertical profiles encountered are shown in Fig. 5 (here the scattering by dry aerosol is in red, whilst the blue traces show the enhanced scattering when relative humidity is taken into consideration – see Sect. 4). There is clearly a general increase in dry AOD from north east to south west across the EUCAARI flight region. The flights to the north and Baltic sea area represent relatively light loadings in a clean air mass before the anticyclonic flow sweeps the air mass south and predominantly eastwards, collecting emissions from north western Europe. Highest AOD values are to be found in the region of Cabauw, heavily influenced by local and cumulative emissions and secondary aerosol formation, including a lot of nitrate which scatters strongly, and to the west of Ireland in the most aged sample, which has again been influenced heavily by emissions contributing to nitrate formation over the UK. Many of the profiles taken over land are incomplete due to restrictions on the minimum altitude permissible for the

ACPD
11, 18487–18525, 2011

aircraft; their lower limit being at 500 m or even higher. Thus the AOD estimated here represents in general a lower limit.

The profiles in Fig. 5 represent the range of vertical structures encountered during EUCAARI (and their positions are marked in Fig. 4). Figure 5a shows profile 8 of B362 (North Sea) and is typical of many profiles performed during the campaign, with the majority of aerosol being below 2000 m in the boundary layer and considerable structure within the BL itself. Morgan et al. (2010b) and Hamburger et al. (2010) give more detailed discussion of the causes of some of this vertical structure. Figure 5b shows a very clean profile encountered over the southern Baltic Sea in B365 where aerosol scattering is only seen in the lowest layers – this is likely to be sea salt. Figure 5c shows an elevated layer of aerosol encountered during profile 16 of B372 – this was observed in profiles off the eastern coast of the UK and the layering reflects local sources below 750m and more aged continental European aerosol above. The peak in scattering at the top of the boundary layer due to enhanced nitrate observed in Morgan et al. (2010b) is seen in Fig. 5d during B374 in the aged pollution over the western Atlantic. Again there is considerable structure throughout the profile below 3000 m, probably corresponding to aerosols from both the UK and the more aged advected European aerosol above.

4 Hygroscopic growth and impact on optical properties

Aerosols are well known to interact with water in the atmosphere, a property which may influence their size, light scattering and chemical reactivity. When an aerosol is dominated by some chemical components, such as nitrate and sulphate, water is easily absorbed by the aerosol causing an increase in size and light scattering (Tang, 1996). Black carbon, on the other hand, is generally understood to have a hydrophobic effect on aerosol. The mixing state of the aerosol and the content of the individual chemical components are critical factors in influencing the hygroscopicity of the aerosol (McMeeking et al., 2011; McFiggans et al., 2005; Gysel et al., 2007). Finally, the

ACPD
11, 18487–18525, 2011

influence of organics on the water uptake of aerosol has been the subject of many studies and this relationship is still not well understood (e.g. Topping et al., 2005)

The wet nephelometer provides a method of probing aerosol hygroscopicity in real time during flights. Aerosol hygroscopicity was characterized by the addition of a second nephelometer (also a TSI 3563) in the inlet line before the "dry" nephelometer (Haywood et al., 2008). The sample flow through this nephelometer is humidified to a set value between 45 and 95 %. During a typical flight the humidity is either cycled through a range between these values or set at a fixed high level (e.g. 80 %). The value f(RH), is defined as the ratio of the "wet" scattering coefficient to the "dry" scattering coefficient. Mean humidograms, showing f(RH) as a function of applied RH were taken for each flight during EUCAARI and fit to an empirical model. In this study, Model 2 taken from Kotchenruther et al. (1999) provided acceptable fits to the data:

$$\sigma_s = \sigma_{s,d}\left(1 + a\left[\frac{RH}{100}\right]^b\right)$$

where $\sigma_{s,d}$, a, and b are fitting parameters to the data. As an example, the humidogram data for flight B374 is shown in Fig. 6. To ensure that the full increase in scattering due to hydration was measured, only data points registering less than 30 % "dry" relative humidity were used. In Fig. 6, the raw data (dots) displays high variability due to small scale variations in f(RH), at a constant RH value (likely an artefact) (Osborne et al., 2006). Thus, the data have been averaged into 2 % mean RH bins.

The fit curves to Model 2 for each flight are shown in Fig. 7 – including corrections for particle loss between the two nephelometers (around 5–10 % on most flights). Many of the flights show largely similar curves. The range of growth curves is spanned by B374 which shows substantially enhanced growth rates, and B365 which shows reduced growth rates. Considering the meteorological situation and location of these flights, this behaviour most likely has a physical explanation – B365 is in relatively clean air over the Southern Baltic Sea – but pollution episodes there contain proportionally much less nitrate and more hydrophobic components than observed further west and

ACPD
11, 18487–18525, 2011

this would result in a shallow growth rate curve. At the other extreme, B374 is the westernmost flight with aged aerosol containing high proportions of nitrates and sulphates – both of which are very hygroscopic. It is appropriate therefore that this growth curve shows most enhancement of scattering across a range of relative humidities. The B367 curve is most markedly different in its hygroscopic behaviour compared to all other flights – this was performed in a very different location (southern Germany) to the other flights and this may be responsible in Southern Germany and this may be responsible for the different hygroscopicity curve. Also shown in Fig. 7 is an average fit using all the individual curves (and an alternative removing the two "outliers" of B367 and B374. The differences between the average fits are small below around 90 % RH and therefore similar under the RH conditions (less than 70 %) experienced during most of the EUCAARI flights. Given the similarity of the flight average curves and the variability within given flights, an average hygroscopicity curve was taken for the entire campaign (a = 1.1475, b = 4.0399). The average curve exhibits modest water uptake, with an f(RH) value of 1.3 at 80 % RH. This is much lower than the value of 2.5 predicted for pure NH_4NO_3 (Tang, 1996), demonstrating a significant contribution of less hygroscopic material (organics and BC). This hygroscopic growth is comparable to other humidograms published in the literature from the UK and European anthropogenic aerosol studies (Haywood et al., 2008).

The impact of relative humidity on optical properties can be seen by increasing the scattering component from the nephelometer by the growth factor indicated from the wet nephelometer campaign average. We assume no influence of humidity on absorption, although Redemann et al. (2001) suggest that absorption can be enhanced by up to 20 % at 80 % RH and by as much as 35 % at 95 % RH. RH experienced during these flights was generally less than 70 % so the effect is likely to be smaller than 20 %. Including the relative humidity effect results in the campaign mean extinction co-efficient being increased by 13 % reaching $5.7 \pm 1.0\,m^2\,g^{-1}$. (Note that here the mass extinction co-efficient is calculated per unit mass of dry aerosol, therefore the value increases on including the effect of relative humidity. If it were defined per unit mass of aerosol

ACPD
11, 18487–18525, 2011

including the mass of water it would decrease).

The ambient SSA is calculated by increasing the scattering value by the growth factor calculated using the wet nephelometer and assuming that the absorption is unaffected by growth due to the relative humidity. Redemann et al. (2001) suggested this assumption led to an overestimate of ambient SSA of up to 0.05 for a narrow size distribution of small particles. There is currently no way to measure this effect on board the BAe-146, but the average RH for the majority of the runs considered here was below 70 % and therefore the effect is likely to be smaller in this study. The ambient SSA and AODs are shown alongside their dry counterparts in Tables 3 and 4 respectively. Generally the influence on SSA is quite small (differences in the average SSA compared to dry value being well within the uncertainty bounds on either quantity). This is due to the relative humidity being generally below 70 %. Figures 6 and 7 show that at this relative humidity the growth of the aerosol is relatively modest and therefore we would not expect dramatic increases in scattering or SSA. For SLRs flown at low level over water (B362 over the North Sea, B365 in southern Baltic Sea and B374 over the Atlantic) a slightly stronger increase in SSA from the dry value is seen as might be expected from a combination of increased RH and the presence of other hygroscopic aerosol such as sea salt.

Figure 4b shows the ambient AOD alongside the dry counterparts with the numerical values given in Table 6. The ratio of ambient to dry AOD is largely determined by the average growth factor curve since scattering is dominant in all profiles and ranges from 1.15 (B373 P7 and B370 P4.2) to 1.43 (B374 P6) suggesting in most profiles a modest increase in aerosol optical depth due to relative humidity. However, the effect on AOD is more marked than that on SSA. Where possible, values of AOD have been compared to those measured on the same day at the nearest AERONET site as indicated on Fig. 4b. Unfortunately in most cases the match to the AERONET station was rather poor either due to distance or due to the presence of air masses of different origin, and the comparison is rather difficult. In all cases the AERONET sites show considerably higher AOD than estimate from aircraft profiles – the measurements are brought into

ACPD
11, 18487–18525, 2011

somewhat better agreement if we assume the maximum 30 % uncertainty in optical depth, but are still an underestimate compared to the AERONET stations. This is not surprising in that the 146 profiles generally do not include the lowest 1000 m which could contain substantial aerosol. In the case of B374 where the profiles do extend much closer to the surface, the AERONET station of Chilbolton is rather distant and under the influence of substantial UK aerosol.

5 Closure experiments

5.1 Scattering and absorption closure for dry aerosol

The scattering and absorption by aerosol mixtures can be calculated using scattering code if the refractive indices and size distribution are known. The refractive indices depend on the composition of the aerosol, and, if wet, the relative humidity. The Aerosol Mass Spectrometer and SP2 instruments on board the FAAM can be used to determine the composition of the aerosol. Detailed discussions of these instruments and the results obtained during the EUCAARI-LONGREX flights can be found for the AMS in Morgan et al. (2010a) and for the SP2 in McMeeking et al. (2010). For this paper, the mass loading of sulphates, organics, nitrates, and black carbon have been used together with volume weighted mixing rules to determine the refractive indices of an internally mixed aerosol having the size distribution measured by the PACSP. Here we discuss the dry aerosol, since the nephelometer and PSAP instruments with which we can perform closure are thought to measure scattering and absorption of dry aerosol (rather than ambient). The assumption of an internally mixed aerosol is valid since in most cases the pollution encountered is aged to some extent. We have assumed refractive indices and densities of the aerosol components as specified in Table 5 (the sensitivity of results to these assumptions is discussed below). Average size distributions as measured by the PCASP for each SLR have been used with these refractive indices and Mie code which assumes a spherical homogenous droplet. The spherical

ACPD
11, 18487–18525, 2011

assumption is appropriate for mixed anthropogenic aerosol, particularly in moderately humid environments; the homogenous droplet assumption may be less appropriate if there is a large mass of black carbon, whereby a coated shell approximation might be more useful. However, in most of the cases considered here, the black carbon mass fraction is small compared to the other components and therefore we consider only the homogenous case.

Figure 8 shows the results of closure studies for scattering (Fig. 8a) and absorption (Fig. 8b). For aerosol scattering, there is remarkably good agreement across all flights with the modelled scattering being within 30 % of the 1:1 relationship – given that the estimated uncertainty in SLR mean scattering is 30 %, this is the best agreement we could envisage. There is a slight bias evident with the modelled value slightly underestimating the measured scattering by around 15 %. Such a bias could be due to several factors. Firstly, if the aerosol being sampled by the nephelometer is not completely dry then the scattering would be slightly increased, however we have tried to correct for that effect in the measurements as described in Sect. 2.2.2. Secondly it is possible that the mass of one or more scattering components is underestimated by the AMS. Thirdly, there is uncertainty in the refractive indices, particularly that for black carbon and organic matter. However, tests varying the refractive indices of black carbon within the range suggested by previous studies have negligible impact on the scattering (not shown) and in any case, the bias is small in relation to uncertainties in nephelometer measurements. The agreement is substantially poorer for absorption. The modelled absorption substantially overestimates the measured absorption for the majority of runs and flights. Flight B368 appears to be an outlier here with very large measured absorbance. The majority or modelled values are at least 50 % higher than their measured counterparts. The average discrepancy of 50 % is not inconsistent with our estimate of uncertainty in measured PSAP values – however, we might have expected the PSAP to over-estimate the absorption by 30–50 % since the organic carbon concentration is relatively high (Lack et al., 2008) and here our model is higher than the PSAP measurement.

ACPD
11, 18487–18525, 2011

Taking into account likely errors in the measured absorption, we must examine reasons why the model could be over-estimating the absorption. The most likely issue concerns the imaginary part of the refractive index for black carbon and/or organic carbon. Considerable debate continues regarding the most appropriate BC refractive index (see e.g. Stier et al., 2007). Figure 9 shows the impact of using two different refractive indices for BC, that in Hess (1998) of 1.77–0.44i (solid squares) and that recommended by Stier et al. (2007) of 1.85–0.71i (solid upright triangles). The use of reduced absorption for BC does bring the modelled and measured absorption closer into agreement, however, the change is modest (less than 20 %). Having far more impact for this study is uncertainty in the imaginary component of the refractive index for organic carbon. Removing all absorption by organic carbon (as suggested in some previous studies) reverses the bias in the model results such that calculated absorption now underestimates the PSAP measurements. In addition, the slope of the dependency is altered for both flights, with the gradient becoming less steep and further from the 1:1 line. Retaining some weak absorption (halving the imaginary refractive index) of OC brings the model and measurements into better agreement in terms of both absolute closure and the gradient of the fit between models and measurements. Therefore we conclude that the organic aerosol measured during this campaign is only moderately absorbing – although perhaps a little more absorbing than the rural HULIS of Dinar et al. (2008), and that this uncertainty is more important for modelling absorption than uncertainties in the BC refractive index. The extent to which this is more widely applicable is limited by the relative amounts of OC and BC in the aerosol. The BC effect is relatively weak here as the mass is relatively small. In regions with high BC loadings, the uncertainty in its absorption is expected to play a far greater role. However, the extent to which we can constrain the refractive indices is limited by the considerable uncertainties in measured absorption.

ACPD
11, 18487–18525, 2011

6 Conclusions

This study suggests that boundary layer aerosol optical properties in anthropogenically perturbed airmasses over western Europe during EUCAARI-LONGREX were described by a mass extinction of 4.96 $m^2 g^{-1}$ (dry) and 5.7 ± 1.0 $m^2 g^{-1}$ (ambient), a single scattering albedo of 0.93 and a scattering growth factor of 1.3. The main regional variations appeared to be the occurrence of relatively high SSA and enhanced growth factor in regions of high nitrate. These led to higher optical depths to the west of the region of study. The role of nitrate in determining optical and hygroscopic properties is of key importance to studies of the radiative effect and forcing of aerosols since many models have yet to include this component. The importance of nitrate in Europe has been confirmed during EUCAARI-LONGREX and may be expected to increase similarly in importance in other regions as sulphate concentrations decline in the future. It is paramount that we include nitrate aerosol in radiative forcing models and have adequate understanding of its optical properties.

Attempts to perform "optical closure" experiments by modelling absorption and scattering derived from chemical composition and size distribution measurements together with assumed refractive indices utilised the new measurements of BC on board the BAe-146 for the first time. It was possible to get good agreement (well within the 30 % measurement uncertainty) between modelled scattering and nephelometer measurements at 550 nm – this suggests that our definition of the real part of the refractive index for the major components of EU aerosol are adequate (at least at this wavelength). However, the agreement for absorption was substantially poorer. Although the agreement to around 50 % was not inconsistent with estimates of uncertainty in the measured absorption, the model consistently appeared to over-estimate the measured absorption (which we expect itself to be an overestimate by some 20–30 %). This strongly suggests that the imaginary part of the refractive index of the absorbing aerosol components used in this study (and others) was too high. Due to the relatively small mass of BC, the influence of uncertainty in BC refractive index was

ACPD
11, 18487–18525, 2011

relatively small here. Reducing the OC absorption to zero did reverse the sign of the bias between model and measurements but also changed the slope of the relationship between model and measurements – pushing it further away from the 1:1 slope. An intermediate value captured both the magnitude and the variation more adequately. It appears that in this region, despite some significant BC sources, it is the secondary aerosol material such as nitrate and oxidised organics that have a major impact on the aerosol optical properties and therefore on radiative effect. It is important to emphasise, however, that this study focussed on the regional scale and therefore is not able to describe conditions near the surface or in urban regions. In those regions and other environments with larger BC mass fraction we would expect the influence of uncertainty in BC refractive index to be larger on the absorption. Indeed, measurements using the same instrumentation in urban outflow suggest that in these regions BC plays a much more important role (McMeeking et al., 2011b).

The SP2 measurements of BC, together with the wet nephelometer and AMS instruments used in this flight campaign offer an enhanced capability for performing optical closure studies across a range of aerosol, giving us the potential to better constrain optical properties and refractive indices used in forcing and climate models. However, in the case of absorbing aerosols, this will not be possible until there are substantial reductions in the uncertainty in absorption measurements – it is of vital importance that research continues into instrumental techniques that can provide the constraint climate models require.

Acknowledgements. This work was supported by NERC ADIENT project NE/E011101/1 and EUCAARI project 036833-2. Airborne data was obtained using the BAe-146-310 large Atmospheric Resesearch Aircraft (ARA) flown by Directflight Ltd and managed by the Facility for Airborne Atmospheric Measurements (FAAM), which is a joint facility of the Natural Environment Researc Council (NERC) and the Met Office. Thanks are also expressed to K. Turnbull for useful discussions regarding instrument corrections.

ACPD
11, 18487–18525, 2011

References

Anderson, T. L. and Ogren, J. A.: Determining aerosol radiative properties using the TSI 3563 integrating nephelometer, Aerosol Sci. Technol., 29, 57–69, 1999.

Bates, T. S., Anderson, T. L., Baynard, T., Bond, T., Boucher, O., Carmichael, G., Clarke, A., Erlick, C., Guo, H., Horowitz, L., Howell, S., Kulkarni, S., Maring, H., McComiskey, A., Middlebrook, A., Noone, K., O'Dowd, C. D., Ogren, J., Penner, J., Quinn, P. K., Ravishankara, A. R., Savoie, D. L., Schwartz, S. E., Shinozuka, Y., Tang, Y., Weber, R. J., and Wu, Y.: Aerosol direct radiative effects over the northwest Atlantic, northwest Pacific, and North Indian Oceans: estimates based on in-situ chemical and optical measurements and chemical transport modeling, Atmos. Chem. Phys., 6, 1657–1732, doi:10.5194/acp-6-1657-2006, 2006.

Bond, T. C. and Bergstrom, R. W.: Light absorption by carbonaceous particles: an investigative review, Aerosol Sci. Technol. 40, 27–67, 2006.

Bond, T. C., Anderson, T. L., and Campbell, D.: Calibration and intercomparison of fliter-based measurements of visible light absorption by aerosols, Aerosol Sci. Technol., 30(6), 582–600, 1999.

Cai, Y. Montague, D. C., and Deshler, T.: Comparison of measuremed and calculated scattering from surface aerosols with an average, size-dependent, and a time-dependent refractive index, J. Geophys. Res., 116, D02202, doi:10.1029/2010JD014607, 2011.

Chylek, P., Srivastava, V., Pinnick, R. G., and Wang, R. T.: Scattering of electromagnetic waves by composite spherical particles: Experiment and effective medium approximations, Appl. Opt., 27, 2396–2404, 1998.

Cook, J., Highwood, E. J., Coe, H., Formenti, P., Haywood, J. M., and Crosier, J.: A comparison of aerosol optical and chemical properties over the Adriatic and Black Seas during summer 2004: Two case-studies from ADRIEX, Q. J. Roy. Meteorol. Soc., 133(S1), 33–45, 2007.

Dinar, E., Mentel, T. F., and Rudich, Y.: The density of humic acids and humic like substances (HULIS) from fresh and aged wood burning and pollution aerosol particles, Atmos. Chem. Phys., 6, 5213–5224, doi:10.5194/acp-6-5213-2006, 2006.

Dinar, E., Abo Riziq, A., Spindler, C., Erlick, C., Kiss, G., and Rudich, Y.: The complex refractive index of atmospheric and model humic-like substances (HULIS) retrieved by a cavity ring down aerosol spectrometer (CRD-AS), Faraday Discuss., 137, 279–295, 2008.

Gysel, M., Crosier, J., Topping, D. O., Whitehead, J. D., Bower, K. N., Cubison, M. J., Williams, P. I., Flynn, M. J., Mcfiggans, G. B., and Coe, H.: Closure study between chemi-

ACPD
11, 18487–18525, 2011

cal composition and hygroscopic growth of aerosol particles during TORCH2, Atmos. Chem. Phys., 7, 6131–6144, doi:10.5194/acp-7-6131-2007, 2007.

Hamburger, T., McMeeking, G., Minikin, A., Birmili, W., Dall'Osto, M., O'Dowd, C., Flentje, H., Henzing, B., Junninen, H., Kristensson, A., de Leeuw, G., Stohl, A., Burkhart, J. F., Coe, H., Krejci, R., and Petzold, A.: Overview of the synoptic and pollution situation over Europe during the EUCAARI-LONGREX field campaign, Atmos. Chem. Phys., 11, 1065–1082, doi:10.5194/acp-11-1065-2011, 2011.

Haywood, J., P. Francis, S. Osborne, M. Glew, N. Loeb, E. Highwood, D. Tanre, G. Myhre, P. Formenti, and E. Hirst, Radiative properties and direct radiative effect of Saharan dust measured by the C-130 aircraft during SHADE: 1. Solar spectrum, J. Geophys. Res., 108(D18), 8577, doi:10.1029/2002JD002687, 2003.

Haywood, J. M., Bush, M., Abel, S., Claxton, B., Coe, H., Crosier, J., Harrison, M., MAcPherson, B., Naylor, M., and Osborne, S: Prediction of visibility and aerosol within the operational Met Office Unified Model. II. Validation of model performance using observational data., Quart. J. Roy. Soc., 134, 1817–1832, 2008.

Hess, M., Koepke, P., and Schult, I.: Opical properties of aerosols and clouds: The software package OPAC, Bull. Am. Met. Soc., 79, 831–844, 1998.

Johnson, D. W., Osborne, S. R., Wood, R., Suhre, K., Johnson, R., Businger, S., Quinn, P. K., Wiedensohler, A., Durkee, P. A., Russell, L. M., Andreae, M., O'Dowd, C., noone, K., Namdy, B., Rudolph, J., and Rapsomanikas, S. : An overview of the Lagrangian experiments undertaken during the North Atlantic Aerosol Characterisation experiments (ACE-2), Tellus, 52B, 290–320, 2000.

Kotchenruther, R. A., Hobbs, P. V., and Heff, D. A.,: Humidifcation factors for atmospheric aerosols off the mid-Atlantic coast of the United States, J. Geophys. Res., 104, 2239–2251, 1999.

Lack, D., Cappa, C., Covert, D., Baynard, T., Massoli, P., Sierau, B., Bates, T., Quinn, P., Lovejoy, E., and Ravishankara, A. R.,: Bias in fliter-based Aerosol Light Absorption Measurements due to Organic Aerosol Loading: Evidence from Ambient Measurements, Aerosol Sci. Tech., 42, 1033–1041, doi:10.1080/02786820802389277, 2008.

McConnell, C. L., Highwood, E. J., Coe, H., Formenti, P., Anderson, B., Osborne, S., Nava, S., Desboeufs, K., Chen, G., Harrison, M. A. J.: Seasonal variations of the physical and optical characteristics of Saharan dust: Results from the dust outflow and deposition to the ocean experiment, J. Geophys., Res., 113, D14S05, doi10.1029/2007JD009606, 2008.

ACPD
11, 18487–18525, 2011

McFiggans, G., Alfarra, M.R., Allan, J., Bower, K., Coe, H., Cubison, M., Topping, D., Williams, P., Decesari, S., Facchini, C., and Fuzzi, S.: Simplification of the representation of the organic component of atmospheric particulates, Faraday Discuss., 130, 341–362, 2005.

McMeeking, G. R., Hamburger, T., Liu, D., Flynn, M., Morgan, W. T., Northway, M., Highwood, E. J., Krejci, R., Allan, J. D., Minikin, A., and Coe, H.: Black carbon measurements in the boundary layer over western and northern Europe, Atmos. Chem. Phys., 10, 9393–9414, doi:10.5194/acp-10-9393-2010, 2010.

McMeeking, G. R., Good, N., Petters, M. D., McFiggans, G., and Coe, H.: Influences on the fraction of hydrophobic and hydrophilic black carbon in the atmosphere, Atmos. Chem. Phys., 11, 5099–5112, doi:10.5194/acp-11-5099-2011, 2011.

McMeeking, G. R., Flynn, M., Morgan, W. T., Highwood, E. J., Turnbull, K., Haywood, J., and Coe, H.: Black carbon aerosol mixing state, organic aerosols and aerosol optical properties over the United Kingdom, manuscript in preparation, 2011a.

Morgan, W. T., Allan, J. D., Bower, K. N., Highwood, E. J., Liu, D., McMeeking, G. R., Northway, M. J., Williams, P. I., Krejci, R., and Coe, H.: Airborne measurements of the spatial distribution of aerosol chemical composition across Europe and evolution of the organic fraction, Atmos. Chem. Phys., 10, 4065–4083, doi:10.5194/acp-10-4065-2010, 2010.

Morgan, W. T., Allan, J. D., Bower, K. N., Esselborn, M., Harris, B., Henzing, J. S., Highwood, E. J., Kiendler-Scharr, A., McMeeking, G. R., Mensah, A. A., Northway, M. J., Osborne, S., Williams, P. I., Krejci, R., and Coe, H.: Enhancement of the aerosol direct radiative effect by semi-volatile aerosol components: airborne measurements in North-Western Europe, Atmos. Chem. Phys., 10, 8151–8171, doi:10.5194/acp-10-8151-2010, 2010.

Ogren, J. A.: Comment on "Calibrations and Intercomparison of fliter-based measurements of Visible Light Absorptino by Aerosols", Aerosol Sci. Tech., 44(8), 589–591, 2010.

Osborne, S. R., Wilson, A., and Rogers, S.: Description and first results of the wet nephelometer fitted to the FAAM BAe-146 research aircraft, OBR Technical Note No. 57, U.K. Met Office, Exeter, 2006.

Osborne, S. R., Haywood, J. M., and Bellouin, N.: In situ and remote-sensing measurements of the mean microphysical and optical properties of industrial pollution aerosol during ADRIEX, Q. J. Roy. Met. Soc., 133(S1), 17–32, 2007.

Quinn, P. K. and Coffman, D. J.: Local closure during the First Aerosol Characterisation Experiment (ACE-1): Aerosol mass concentration and scattering and backscattering coefficients, J. Geophys. Res., 103, 16575–16596, 1998.

ACPD
11, 18487–18525, 2011

Redemann, J., Russell, P. B., and Hamil, P.: Dependence of light absorption and single-scattering albedo on ambient relative humidity for sulfate aerosols with black carbon cores, J. Geophys. Res., 106, 27485–27495, 2001.

Schwarz, J. P., Gao, R. S., Fahey, D. W., Thomson, D. S., Watts, L. A., Wilson, J. C., Reeves, J. M., Darbeheshti, M., Baumgardner, D. G., Kok, G. L., Chung, S. H., Schulz, M., Hendriks, J., Lauer, A., Karcher, B., Slowik, J. G., Rosenlof, K. H., Thompson, T. L., Langford, A. O., Lowenstein, M., and Aiken, K. C.: Single particle measurements of mid-latitude black carbon and light-scattering aerosols from the boundary layer to the lower stratosphere, J. Geophys. Res., 110, D16207, 2006.

Sciare, J., Oikonomou, K., Cachier, H., Mihalopoulos, N., Andreae, M. O., Maenhaut, W., and Sarda-Estve, R.: Aerosol mass closure and reconstruction of the light scattering coefficient over the Eastern Mediterranean Sea during the MINOS campaign, Atmos. Chem. Phys., 5, 2253–2265, doi:10.5194/acp-5-2253-2005, 2005.

Stephens, M., Turner, N, and Sandberg, J.: Particle identification by laser-induced incandescence in a solid-state laser cavity, Appl. Optics, 42(19), 3726–3736, 2003.

Stier, P., Seinfeld, J. H., Kinne, S., and Boucher, O.: Aerosol absorption and radiative forcing, Atmos. Chem. Phys., 7, 5237–5261, doi:10.5194/acp-7-5237-2007, 2007.

Tang, I. N.: Chemical and size effects of hygroscopic aerosols on light scattering coefficients, J. Geophys. Res., 101, 19245–19250, 1996.

Toon, O. B., Pollack, J. B., and Khare, B. N.: The optical constants of several atmospheric aerosol species: ammonium sulphate, aluminium oxide and sodium chloride, J. Geophys. Res., 81, 5733–5748, 1996.

Topping, D. O., McFiggans, G. B., and Coe, H.: A curved multi-component aerosol hygroscopicity model framework: Part 1 - Inorganic compounds, Atmos. Chem. Phys., 5, 1205–1222, doi:10.5194/acp-5-1205-2005, 2005.

Turnbull, K.: PSAP Corrections: Amendment to MRF Technical Note No. 31., OBR Technical Note, No. 80, Met Office, August 2010.

Weast R.C. (Ed.): CRC Handbook of Chemistry and Physics (67th edn.), CRC press: Boca Raton, Florida, 1986.

Wex, H., Neususs, C., Wendisch, M., Stratmann, F., Koziar, C., Keil, A., Wiednsohler, A., Ebert, M.: Particle scattering, backscattering and absorption co-efficients: An in-situ closure and sensitivity study, J. Geophys. Res. 107(D21), 8122, doi:10.1029/2000JD000234, 2002.

ACPD
11, 18487–18525, 2011

Table 1. Flights from May 2008 used in EUCAARI analysis. Classification according to Morgan et al. (2009): L1 = LONGREX-1, L2 = LONGREX-2, L3 = LONGEX-3.

Flight number	Date and classification	General location	Comments
B362	6 May, a.m. (L1)	Germany/Belgium and N. Sea	
B363	6 May, p.m. (L1)	Germany/Belgium and N. Sea	
B364	7 May, p.m. (L1)	Southern Germany	
B365	8 May (L1)	Eastern Europe and the Baltic Sea	
B366	8 May (L1)	North-western Europe	PCASP QA failure*
B367	9 May	Southern Germany	DLR intercomparison flight
B368	10 May, a.m. (L2)	Germany/Poland and Baltic coast	
B369	10 May, p.m. (L2)	Baltic Sea/Germany	
B370	12 May, a.m. (L2)	Germany, Netherlands and N. Sea	
B371	12 May (L2)	Germany/Baltic Sea	
B372	13 May, a.m. (L2)	Germany/Poland/Netherlands/ East coast of UK	No BC data*
B373	13 May, a.m. (L2)	Southern UK coast	
B374	14 May (L2)	Irish sea and Atlantic ocean SW of Ireland	
B379	21 May (L3)	Germany/Netherlands/Belgium	
B380	22 May (L3)	Germany/Netherlands/Belgium and Southern UK coast	

* not used for closure studies in Sect. 5.

ACPD
11, 18487–18525, 2011

Table 2. Overview of measurements made on board the FAAM BAe-146 utilised in this study.

Parameter	Instruments	Comments/Corrections
Aerosol size distribution 15 size bins 0.1–3 µm diameter	Wing pod mounted Particle Measuring System passive cavity aerosol spectrometer probe 100-X (PCASP)	Laboratory calculations to characterize bin widths. No corrections made for refractive index
Aerosol scattering coefficients at 440, 550 and 700 nm	TSI 3563 nephelometer.	Corrected for angular truncation and temperature and pressure according to Anderson and Ogren (1998); Turnbull (2010).
Aerosol absorption coefficient at 567 nm	Radiance Research particle soot absorption photometer (PSAP).	Adjustment from 567 nm to 550 nm, pressure/flow corrections, and corrections for spot size as outlined in previous studies (Bond et al., 1999; Turnbull, 2010)
Chemical composition: total non-refractory mass in groups of chemical composition (e.g. organics, nitrate, sulphate, ammonium and chloride)	Aerodyne time-of-flight aerosol mass spectrometer (ToF-AMS)	Only particles less than about 800 nm aerodynamic diameter are sampled by the instrument. See Morgan et al. (2010a).
Black carbon mass (measures black carbon by incandescence of individual particles)	Single particle soot photometer (SP2).	Described in detail by Schwarz et al. and in the context of ADIENT by McMeeking et al. (2010)

ACPD
11, 18487–18525, 2011

Table 3. Flight averaged SSA values for aerosol derived from PSAP and nephelometer for dry and ambient (scattering corrected for relative humidity measured during run) aerosol. LOWLEV is mean of SLRs below 250 m, BL is mean of all SLRs between 250 m and 2000 m, numbers in brackets in the dry columns describe number of runs used to calculate the mean in each case. Where there is no entry in the table, no runs were made in that height region.

Flight number	LOWLEV		BL	
	DRY	AMBIENT	DRY	AMBIENT
B362	0.96 (1)	0.97	0.94 (10)	0.95
B363			0.94 (5)	0.95
B364			0.93 (4)	0.94
B365	0.96 (1)	0.96	0.91 (6)	0.93
B366			0.93 (6)	0.94
B367			0.92 (2)	0.92
B368			0.70 (6)	0.72
B369	0.93 (2)	0.94	0.92 (4)	0.92
B370			0.94 (4)	0.95
B371			0.92 (6)	0.94
B373			0.93 (8)	0.93
B374	0.94 (2)	0.96	0.93 (3)	0.94
B379			0.94 (5)	0.95
B380	0.90 (1)	0.90	0.94 (6)	0.95
MEAN	**0.94**	**0.94**	**0.91**	**0.92**
(ex B368)	**0.94**	**0.94**	**0.93**	**0.94**

ACPD
11, 18487–18525, 2011

Table 4. Optical depths at 550 nm calculated from the most complete scattering profiles for dry and ambient aerosol (scattering corrected using the measured growth factor). AERONET aerosol optical depths are shown as daily averages for the closest station and have been scaled to 550 nm assuming an inverse relationship with wavelength (Ch – Chilbolton, CB – Cabauw, HA – Hamburg).

Flight	Profile	Approximate Altitude Range (m)	AOD (dry)	AOD (ambient)	AOD Aeronet Location code
B362	P8	0–3048	0.082	0.106	
	P9/P10	0–3048	0.076	0.092	
B365	P6	1000–8000	0.120	0.169	
	P7/P8	500–3700	0.054	0.083	
B370	P4.2	700–3500	0.072	0.083	0.179 HA
B372	P16	400–4500	0.080	0.103	
B373	P7	0–3000	0.138	0.158	
B373	P13	0–3300	0.116	0.141	
B374	P6	0–6000	0.194	0.278	0.448 CH
	P12	0–7000	0.168	0.212	
B379	P5/P6/P7/P8	500–8500	0.148	0.198	0.261 CB

ACPD
11, 18487–18525, 2011

Table 5. Refractive indices and densities used for aerosol components in calculation of mixture density and refractive index for input to Mie calculations.

Component	Refractive indices at 550 nm	Density (gcm^{-3})	References
Ammonium Sulfate $(NH_4)_2SO_4$	1.53–0i	1.77	Toon (1976)
Organic carbon (Swannee River Fulvic Acid)	1.538–0.02i	1.5	Dinar et al. (2006, 2008)
Black carbon	1.95–0.79i	1.80	Bond and Bergstrom (2006)
Ammonium nitrate (NH_4NO_3)	1.611–0i	1.80	Weast (1966) as cited in Cook et al. (2004)
Sodium chloride	1.5-1e-08	2.20	

ACPD
11, 18487–18525, 2011

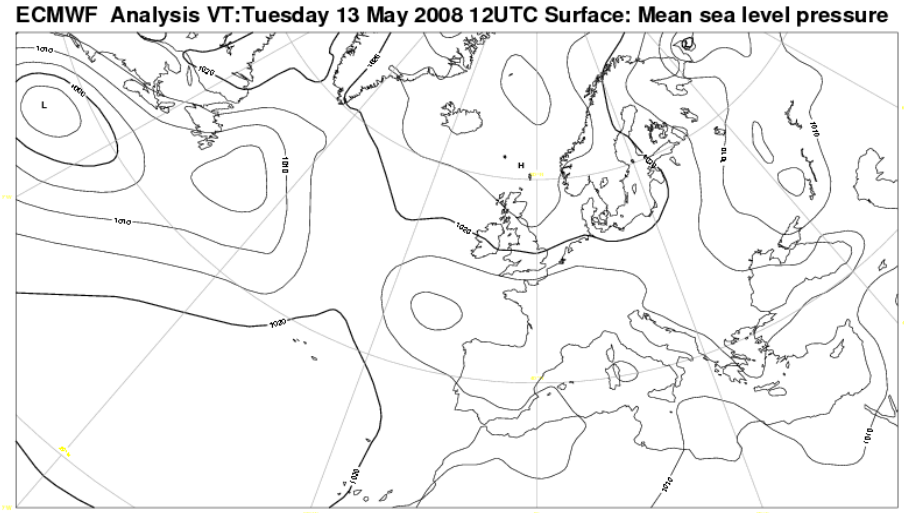

Fig. 1. Mean sea-level pressure from ERA-Interim data on 13 May 2008 during LONGREX-2 period.

ACPD
11, 18487–18525, 2011

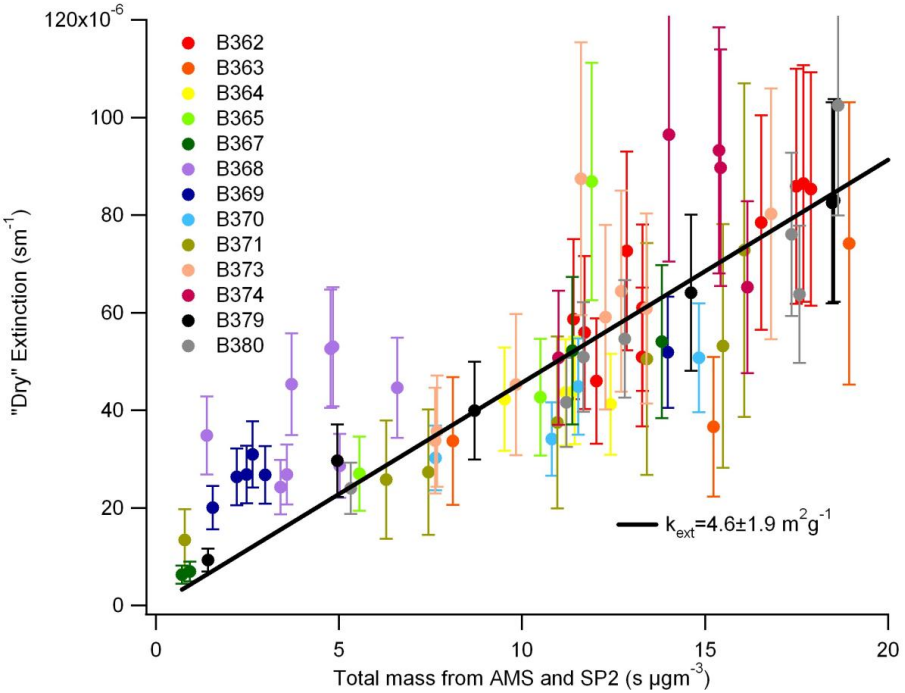

Fig. 2. Aerosol extinction as calculated as the total of scattering measured by the nephelometer and absorption measured by PSAP as a function of total aerosol mass (from total of Aerosol Mass Spectrometer and SP2 instrument). Error bars are uncertainty as calculated from measurement errors and in-run variability of scattering and absorption (one standard deviation) for each individual run. Solid line represents a mass extinction relationship of $4.56 \pm 1.9\,m^2\,g^{-1}$ (uncertainty is the average residual from the best-fit line). All quantities reported at standard temperature and Pressure (STP).

ACPD
11, 18487–18525, 2011

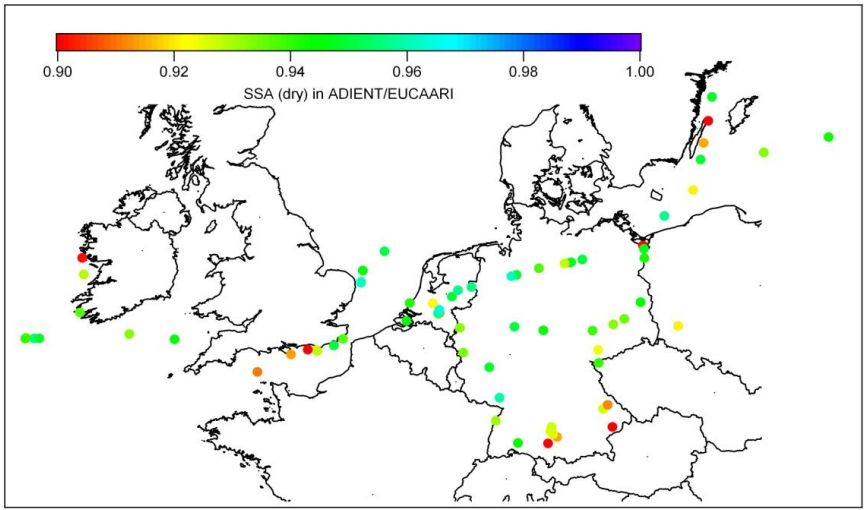

Fig. 3. Single scattering albedo (SSA) of dry aerosol as derived from PSAP and nephelometer measurements on board the BAe146. Markers are positioned at the mid-points of the SLRs. Only SLRs below 2000 m (i.e. within the average boundary layer) are included as the aerosol concentrations drop rapidly above the boundary layer leading to large uncertainties in the scattering and absorption measurements.

ACPD
11, 18487–18525, 2011

a)

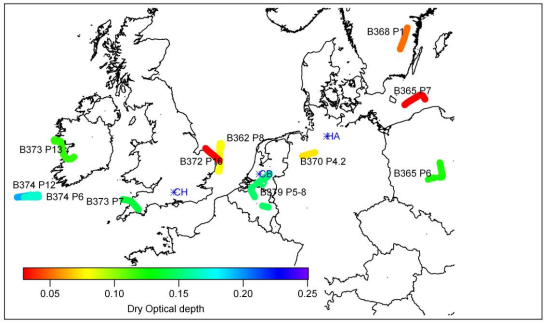

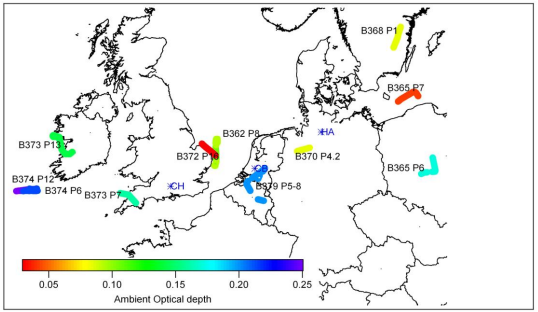

b)

Fig. 4. showing **(a)** dry aerosol optical depth and **(b)** ambient optical depth for deep profiles flown during EUCAARI. The locations of AERONET stations used in comparison for Table 4 are also shown as follows: CH – Chilbolton, CB – Cabaux, HA – Hamburg.

ACPD
11, 18487–18525, 2011

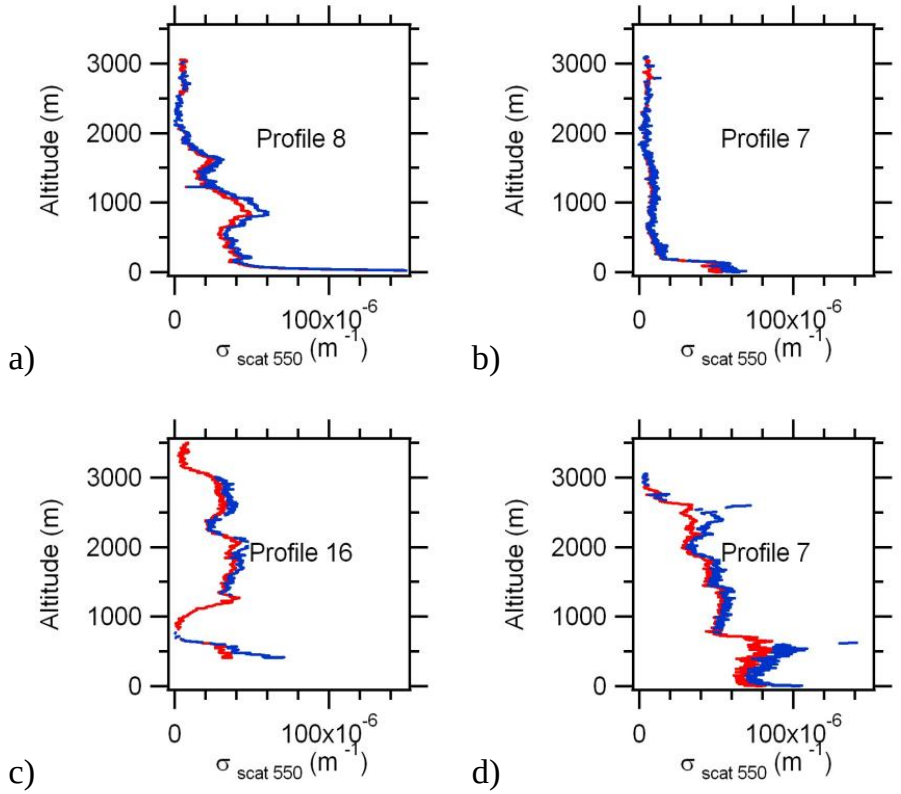

Fig. 5. Example profiles of scattering from the EUCAARI campaign. **(a)** Profile 8 from B362; **(b)** profile 7 from B365, **(c)** profile 16 from B372 and **(d)** profile 7 from B373. Dry aerosol scattering – red, scattering at ambient relative humidity – blue.

ACPD
11, 18487–18525, 2011

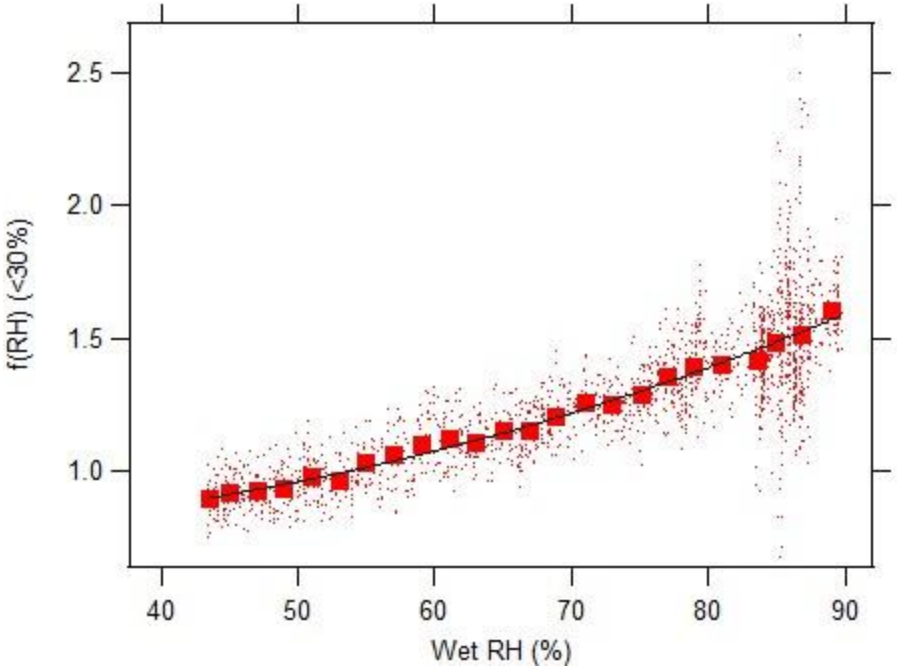

Fig. 6. Humidogram constructed using the wet nephelometer measurements for the entire flight of B374, showing all data (dots), 2 min averages (red squares) and the Model 2 fit to the data (black line).

ACPD
11, 18487–18525, 2011

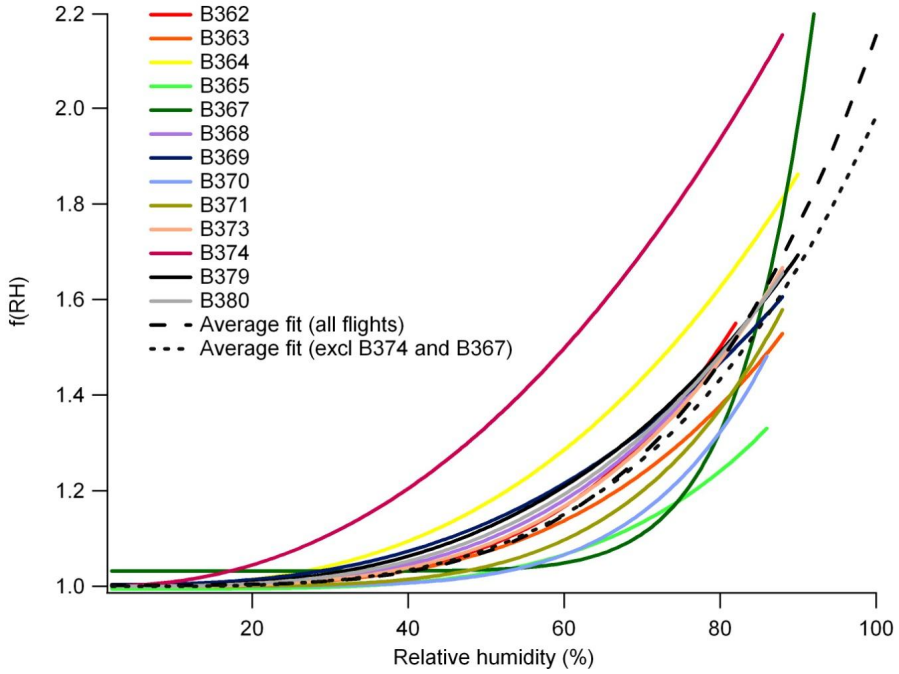

Fig. 7. Growth curves derived from the wet nephelometer and averaged over each flight. Solid dashed line – average fit calculated using all flights. Solid dotted line, average fit excluding B374 and B367.

ACPD
11, 18487–18525, 2011

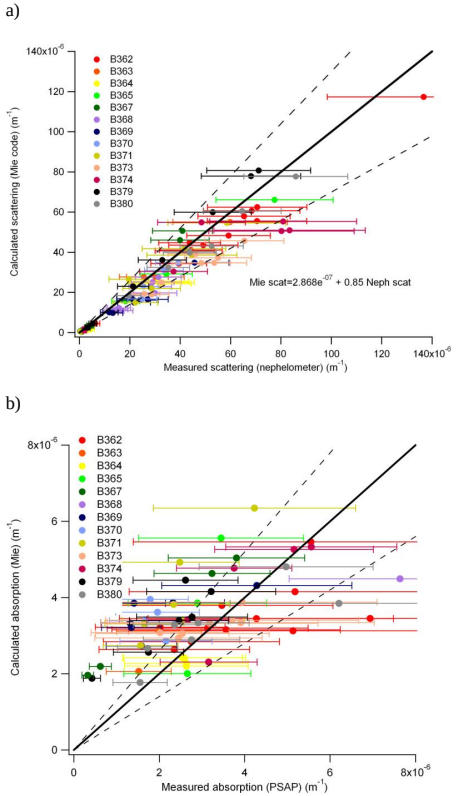

Fig. 8. Calculated versus measured scattering **(a)** and absorption **(b)** averaged for each run in every flight from EUCAARI-LONGREX. The one-to-one line is indicated (solid black) as are the +/−30 % tolerances (dashed lines). Error bars show the uncertainty in measured scattering assuming a measurement uncertainty of 20 % for the nephelometer and in-run variability ranging from 12–35 % in **(a)** and the uncertainty in measured absorption assuming a measurement uncertainty of 30 % for the PSAP and in-run variability ranging from 16–47 % in **(b)**. Parameters for a linear best fit are also indicated for scattering comparison.

ACPD
11, 18487–18525, 2011

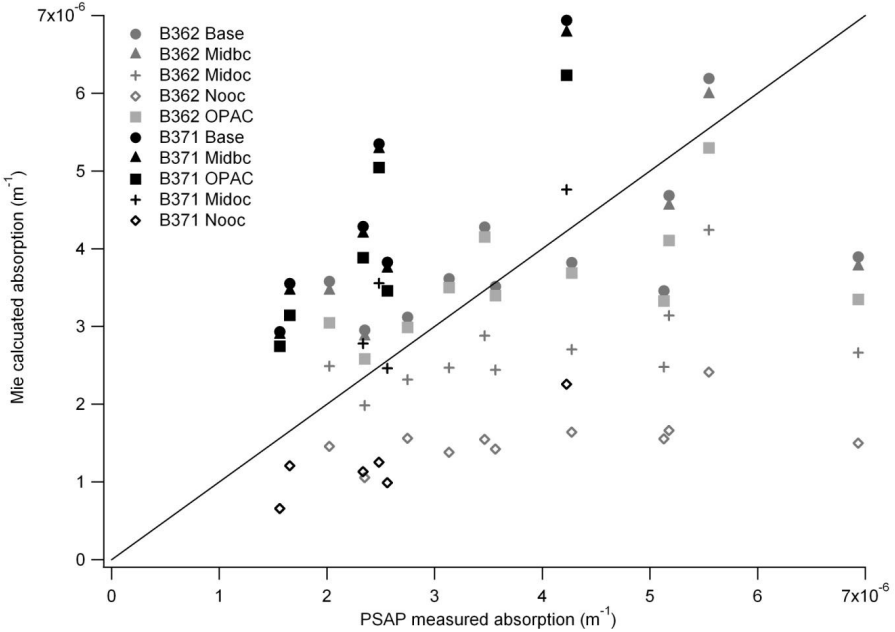

Fig. 9. Sensitivity of absorption closure to assumptions in refractive index of absorbing components for flights B362 and B371. Base is the control simulation as used elsewhere in the paper. OPAC refers to BC refractive indices from Hess et al. (1998), Midbc is the value from Stier et al. (2007). "Nooc" is a simulation with no absorption by organic carbon, whilst "Midoc" refers to an imaginary component for OC of 0.105 (half that in the Base case).

ACPD
11, 18487–18525, 2011